J. Membrane Biol. 175, 9–16 (2000)

The Journal of
Membrane
Biology



# Diffusion of Small Solutes in the Lateral Intercellular Spaces of MDCK Cell Epithelium Grown on Permeable Supports

**O.N. Kovbasnjuk[1], P.M. Bungay[2], K.R. Spring[1]**

[1]Laboratory of Kidney and Electrolyte Metabolism, National Heart, Lung and Blood Institute, Bethesda, MD 20892-5766, USA
[2]Bioengineering and Physical Science Program, Office of Research Services, National Institutes of Health, Bethesda, MD 20892-5766, USA

Received: 7 October 1999

**Abstract.** The diffusion coefficients of four solutes ranging in molecular weight from 238 to 10,000 in the lateral intercellular spaces (LIS) of cultured kidney cells (MDCK) grown on permeable supports were determined from the spread of fluorescence produced after the release of caged compounds by a pulse from a UV laser. Two types of experiments were performed: measurement of the rate of change of fluorescence after releasing a caged fluorophore, and measurement of the change in fluorescence of a relatively static fluorescent dye produced by the diffusion of an uncaged ligand for the dye. Fluorescence intensity was determined by photon-counting the outputs of a multichannel photomultiplier tube. Diffusion coefficients were determined in free solution as well as in the LIS of MDCK cells grown on permeable supports and the hindrance factor, $\theta$, determined from the ratio of the free solution diffusivity to that in the LIS. The hindrance factors for 3000-MW dextran, 8-hydroxypyrene-1,3,6-trisulfonic acid (HPTS, MW 524) and N-2-hydroxyethylpiperazine-N′-2-ethanesulfonic acid (HEPES, MW 238) were not significantly different from 1. The diffusion of 10,000-MW dextran was substantially reduced in the LIS with a $\theta$ of $5.6 \pm 0.3$. Enzymatic digestion by neuraminidase of the sialic acid residues of the glycosylation groups in the LIS increased the diffusivity of the 10,000-MW dextran 1.8-fold indicating hindrance by the glycocalyx. We conclude that small solutes, such as $Na^+$ and $Cl^-$, would not be significantly restricted in their diffusion in the LIS and that solute concentration gradients could not develop along the LIS under physiologic conditions.

**Key words:** Caged compound — HEPES — Dextran — Fluid transport — Caged protons — Neuraminidase

*Correspondence to:* K.R. Spring

## Introduction

The mechanism of isosmotic fluid absorption by epithelia remains a subject of controversy (Spring, 1999). Most mathematical models of fluid transport assign the coupling of solute and water movements to the lateral intercellular spaces (LIS) separating the epithelial cells and assume restricted solute diffusion within the LIS to permit the development of osmotic gradients along the length of the LIS. The diffusion coefficients of two solutes, a 10,000-MW fluorescein dextran and 8-hydroxypyrene-1,3,6-trisulfonic acid (HPTS, 524 MW) were previously determined in the LIS of MDCK cell epithelia grown on glass coverslips (Xia et al., 1998). This study showed that while the diffusivity of HPTS in the LIS was similar to that in free solution, the larger dextran was restricted 1.6-fold in its diffusion compared to free solution. It was concluded that the lack of restriction to the diffusion of small solutes, such as HPTS, was not consistent with mathematical models in which solute gradients developed. This investigation utilized MDCK cells grown on glass coverslips, a less physiologic situation than the culture of the cells on permeable supports. Diffusional limitations might be present in MDCK cells grown on permeable supports because these cells are taller and develop more elaborate LIS than those grown on glass coverslips (Chatton & Spring, 1994).

In the present study, we determined the diffusion coefficients of four solutes ranging in molecular weight from 238 to 10,000 within the LIS of MDCK cells grown on permeable supports. As in the previous study (Xia et al., 1998), caged compounds were employed. In addition, we developed a method for the determination of the diffusivity of caged, nonfluorescent solutes that act as a ligand for an immobilized fluorescent dye. To this end, we utilized the release of caged protons to determine the diffusion coefficient of N-2-hydroxyethylpiperazine-N′-

2-ethanesulfonic acid (HEPES) when the LIS was filled with a pH-sensitive, fluorescently labeled, high molecular weight dextran. Our results show that the diffusion in the LIS of small solutes, such as HPTS and HEPES, is not substantially restricted in MDCK cells grown on permeable supports.

## Materials and Methods

### Cell Culture and Perfusion System

Low-resistance MDCK cells (passages 69–82 from the American Type Culture Collection, Rockville, MD) were maintained as previously described (Harris et al., 1994), using Dulbecco's modified Eagle medium (DMEM) plus 10% fetal bovine serum (Gibco, Grand Island, NY) and 2 mM glutamine, but without riboflavin, antibiotics, or phenol red. For experimental purpose the cells were grown to confluence on 24-mm diameter Anocell membranes (Whatman, Clifton, NJ) that had been treated to reduce pore size sufficiently (Chatton & Spring, 1994) to be effectively impermeable to the fluorescent and caged markers.

Monolayers were perfused with HEPES-buffered solution at 37°C in a bilateral perfusion chamber mounted on the stage of the microscope. The perfusion medium contained (in mM): 14 HEPES, 142 Na, 5.3 K, 1.8 Ca, 0.8 Mg, 136.9 Cl, 5.6 glucose. In experiments utilizing the caged protons, the perfusion solution was similar in composition except that it contained 1 mM HEPES.

### Chemicals

2,7-biscarboxyethyl-5,6-carboxyfluorescein dextran (BCECF dextran, MW 70,000), fluorescein dextran (MW 70,000) and caged probes: 8-((4,5-dimethoxy-2-nitrobenzyl)oxy)pyrene-1,3,6-trisulfonic acid, trisodium salt (DMNB-caged HPTS); (4,5-dimethoxy-2-nitrobenzyl)fluorescein dextrans (MW 10,000; MW 3,000); and 2-hydroxyphenyl-1-(2-nitrophenyl)ethyl phosphate, sodium salt (NPE-caged proton) were obtained from Molecular Probes (Eugene, OR). Neuraminidase (type V from *Clostridium perfringens*) was purchased from Sigma (St. Louis, MO).

### Perfusion Chamber

The Anocell filters with adherent cells were loaded into a bilateral perfusion chamber, as described previously (Chatton & Spring, 1994). The perfusion chamber was maintained at 37°C, and the rate of perfusion was controlled by hydrostatic pressure as previously described (Chatton & Spring, 1994).

### Loading Dye and Caged Compounds into the LIS

Caged compounds and fluorescent dye were microinjected into the MDCK monolayers as previously described (Kovbasnjuk et al., 1998). Briefly, a sharpened glass micropipette (1-μm diameter) filled with HEPES buffer solution containing 1 mM caged fluorescent dye (or mixture of 0.5 mM NPE-caged proton and 0.5 mM BCECF dextran or fluorescein dextran) was used to inject the solution between the epithelium and the permeable support at several locations. Over the next few min the injected dye or caged compounds diffused from the puncture sites into the LIS of adjacent undisturbed regions of the monolayer and remained trapped in the LIS for the duration of the experiments. The area selected for experimental measurements was at least 3–4 cells away from any injection site.

### Fluorescence Microscopy

The experiments were performed on the stage of an inverted microscope (Diaphot, Nikon, Melville, NY) modified for simultaneous transmitted light differential interference contrast (DIC) and low light level fluorescence as previously described (Xia et al., 1998). For fluorescence excitation, a beam from multiline argon laser passed through an acousto-optical tunable filter to produce light output at 458 or 488 nm and was launched into a multimode fused silica optical fiber and directed by dichromatic mirrors to a 100×/1.3 N.A. objective lens (Nikon). The resultant beam formed a 24-μm-radius uniformly illuminated spot in the microscopic field.

### Uncaging Illumination and Detection Systems

The system configuration for photoactivation of caged probes was described in detail previously (Spring et al., 1998; Xia et al., 1998). Briefly, the photocleavage of the caged compounds in a small region of microscopic field was accomplished by a 5-nsec pulse of light at 355 nm directed through a 1-mm pinhole to improve beam geometry and then reflected by a dichromatic mirror to the epi-illumination port of the microscope. The 355-nm beam was centered in the excitation field, and was reflected by the dichromatic mirror in the microscope nosepiece to the objective. The resultant low numerical aperture beam formed a 1.5-μm-radius uniform spot at the image plane. The fluorescence emission light was divided equally between an intensified CCD camera and a 64-channel photomultiplier tube, operated in the photon counting configuration with simultaneous readout of all channels in parallel. The maximum sampling rate for the PMT was 1 kHz with a dark count of 0.05–0.1 counts/sample. Each PMT corresponded to a region of 10 × 10 μm in the image plane. Customized software was developed that permitted acquisition of data before and after an uncaging pulse and subsequent plotting of selected channels.

### Statistics

Data are presented as mean ± SEM. Statistical significance was determined using the paired or unpaired *t*-test, and *P* value less than 0.05 was considered significant. Multiple comparisons were made by analysis of variance followed by application of the Bonferroni Multiple Comparisons Test.

### Data Analysis

The small uncaging spot size allowed us to assume that diffusion of both the caged and uncaged species could be neglected in the approximately 5-nsec uncaging interval. Diffusion coefficients in the LIS were compared to the apparent free solution value determined from a thin (~10 μm) film of dye in perfusion solution trapped between a clean coverslip and glass slide. The hindrance factor, θ, was calculated as the ratio of the free solution diffusion coefficient to that measured for the probe in the LIS. In addition, the fraction of caged protons released by a single laser pulse was estimated by mixing the experimental solution with 85–90% glycerin to impede diffusion.

### Uncaging of Diffusible Dye in a Thin Film

We assume that uncaged dye diffuses freely in the radial direction and dye concentration is uniform in the transverse direction, since the uncaging beam diameter is virtually unchanged in the 10-μm z-axis distance corresponding to the thin film thickness. As shown in Eq. 1, the fluorescence of the released dye after uncaging, $F[t]$, measured by the PMT channel corresponding to the release site is a function of time, $t$, the fluorescence at long times after uncaging, $F^{\infty}$, the effective diffusion coefficient, $D_{eff}$, the uncaging beam radius, $\rho_u$, and the equivalent radius of the PMT sensor, $\rho_s$.

$$F[t] = F^{\infty} - F^{ref}\frac{1 - \exp^{-}\left(\frac{\left(\frac{\rho_s}{\rho_u}\right)^2}{1 + 4D_{eff}\frac{t}{\rho_u{}^2}}\right)}{\left(\frac{\rho_s}{\rho_u}\right)^2}, \quad (1)$$

in which $F^{ref}$ is a constant determined by the initial reactant concentrations.

### Uncaging Within a Small Region of LIS

Uncaging was confined to selected straight and narrow segments of LIS and it was assumed that diffusion from the release site could be treated as rectilinear, instead of radial. As in the case of the thin film, transverse beam geometry was assumed uniform in the 6–8 μm corresponding to the height of an MDCK cell. The only diffusion considered in the post-uncaging period was that of the uncaged dye or of its reaction product (*see below*). For rectilinear diffusion of uncaged dye out of the central channel, the fluorescence at any time, $F[t]$, is given by

$$F[t] = F^{\infty} - F^{ref}\frac{erf\left(\frac{\left(\frac{\rho_s}{\rho_u}\right)}{\sqrt{1 + 4D_{eff}\frac{t}{\rho_u{}^2}}}\right)}{\left(\frac{\rho_s}{\rho_u}\right)}. \quad (2)$$

The diffusion coefficients were evaluated using equations 1 and 2 by Marquardt-Levenberg nonlinear regression. Instead of a square PMT area of dimension 10 μm × 10 μm, the sense area was treated as a circular region with a radius, $\rho_s$, equal to 5.6 μm, the value for an equivalent area. The parameters $Fi^{\infty}$, $F^{ref}$, and the diffusion coefficient, $D_{free}$, were simultaneously estimated by regression. Fluorescence was sampled every 2 msec.

### Uncaging Protons for Estimation of HEPES Diffusion

In this situation, both NPE-caged proton and high molecular weight fluorescein or BCECF dextran were added to a weakly buffered perfusion solution containing 1 mM HEPES. It is assumed that protons released by the uncaging pulse react rapidly with available with available unprotonated HEPES and the fluorescein-dextran. We also assume that the diffusion of protonated HEPES dominates the time course of the fluorescence signal that is sensed by the PMT array. As protonated HEPES spreads from the release site and encounters higher pH regions, it releases protons that react with groups on the fluorescein or BCECF dextrans, thereby reducing the fluorescence of these molecules. The rate of spread of the altered fluorescence signal is not only a function of HEPES diffusion but also of proton diffusion and the reaction kinetics for the three species as well as of their relative concentrations. Our attempts to quantitatively model this complex situation in thin films were unsuccessful, and we chose to simply compare the rate of spread of fluorescence observed in thin films with that seen in the LIS assuming that the thin film rates represented the "free solution" value for HEPES diffusion. In principle, severe restrictions to proton diffusion (e.g., more than a 100-fold reduction) would also be detectable as a slowing of apparent HEPES diffusion.

## Results

Three different molecular weight caged fluorescence dyes were chosen to measure the dye diffusion from a 1.5-μm radius uncaging region of the LIS of MDCK cells grown on permeable supports. Fluorescence intensity before and after a dye release from caged compound was detected by PMT at a sampling rate of 500 Hz. For these experiments the signal from the PMT channel coinciding with the uncaging beam site was selected.

### Fluorescein Dextran and HPTS Diffusion Measurements

The temporal fluorescence intensity profile for the uncaging of 10,000-MW fluorescein dextran is illustrated in Fig. 1 (top). The diffusion coefficient value was obtained from the best-fit simulation using the nonlinear regression. The mean ± SEM for the diffusion coefficient of 10,000-MW dextran in 22 measurements in the LIS at 37°C was $1.8 \pm 0.3 \times 10^{-7}$ cm$^2$/sec. The corresponding hindrance factor, θ, based on the previously determined diffusion coefficient in free solution ($9.8 \pm 0.6 \times 10^{-7}$ cm$^2$/sec; Xia et al., 1998) is 5.6 ± 0.3 (significantly different from 1.0, $P < 0.01$).

Figure 1 (middle) shows a typical record for the 3,000-MW fluorescein dextran diffusion within the LIS. The mean ± SEM for the diffusion coefficient of 3,000-MW dextran at 37°C was $1.8 \pm 0.4 \times 10^{-6}$ cm$^3$/sec ($n = 7$), an order of magnitude higher than for 10,000-MW dextran. The measured diffusion coefficient of this dye in free solution at 37°C was $1.4 \pm 0.04 \times 10^{-6}$ cm$^2$/sec ($n = 12$), yielding a hindrance factor of $\theta = 0.77 \pm 0.16$, not significantly different from 1.0.

Figure 1 (bottom) shows a typical record of HPTS diffusion within the LIS. The mean ± SEM for the diffusion coefficient of HPTS at 37°C was $4.4 \pm 0.1 \times 10^{-6}$ cm$^2$/sec ($n = 19$). The measured diffusion coefficient for this dye in free solution at 37°C was $4.6 \pm 0.4 \times 10^{-6}$ cm$^2$/sec ($n = 8$), yielding a $\theta = 1.04 \pm 0.09$ (not significantly different from 1.0).

### HEPES Diffusion

Because all three caged dyes shown in Fig. 1 are anions, we sought an approach for the determination of the dif-

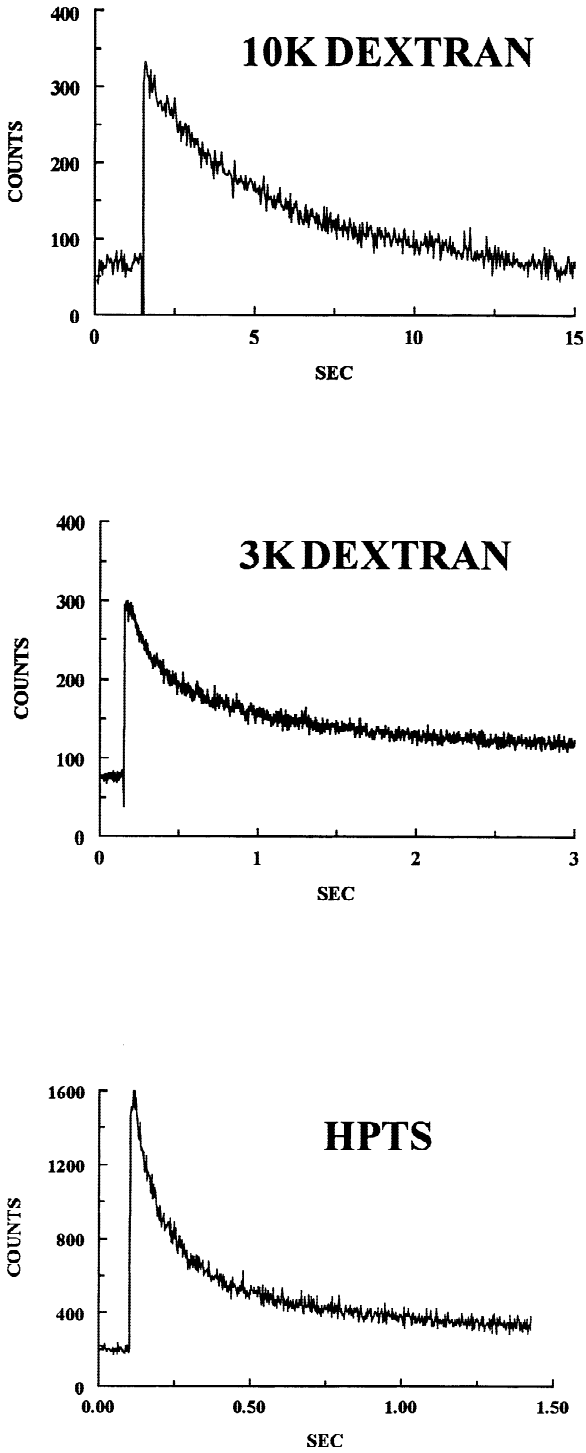


**Fig. 1.** Uncaging of three solutes in the LIS of MDCK cells. Photon counts from the PMT channel corresponding to the uncaging site is shown on the ordinate with time on the abscissa. Note the different time scales for each solute. Fifty samples were taken prior to the uncaging pulse, corresponding to 2 sec in the top panel (10 K Dextran), 0.2 sec in the middle panel (3 K Dextran), and 0.1 sec in the bottom panel (HPTS).

fusivity of a cation in the LIS. We ruled out measurements of abundant cations, such as $Na^+$ or $K^+$, because caged species were not available and very large concentration changes would be required for effective sensing by fluorescent indicators. Caged protons provided the only cationic solute whose diffusion could be feasibly measured in the LIS as a relatively small change in proton concentration can be readily detected. We developed a method for determining the localized pH change that occurred when protons were suddenly released by uncaging. Localized pH changes altered the fluorescence of the pH-sensitive dyes fluorescein or BCECF attached to a 70,000-MW dextran. For all practical purposes the dye-dextran was immobile during the time of the pH transient. The buffer concentration of the perfusion solution was reduced so that the sudden jump in proton concentration produced by uncaging would result in a large pH decrease at the uncaging site. The optimum experimental circumstances were determined on thin films of solution trapped between glass coverslips and a glass slide. A perfusion solution containing 0.5 mM NPE-caged protons, 1 mM HEPES, and 0.5 mM fluorescein-70,000-MW dextran proved to be suitable.

First, the fraction of NPE-caged protons released by a single 5-nsec laser pulse was determined by mixing the caged compound, dye-dextran and HEPES with 85–90% glycerin to minimize lateral diffusion in the thin film. These experiments showed that approximately 85% of the NPE-caged protons were released by a single pulse. Subsequent pulses uncaged the remaining protons. Thus, the calculated proton concentration within the 1.5-μm radius uncaging beam increases by 0.43 mM after a single pulse. At the perfusate pH of 7.4, approximately half (0.51 mM) of the HEPES is protonated as the HEPES pK is 7.52. In free solution, the remaining HEPES (0.49 mM) should be rapidly protonated at the uncaging site and then diffuse away. The pK of fluorescein-dextran is 6.4 and each dextran contains 6 fluoresceins, so any remaining free protons should bind immediately to the available fluoresceins (calculated dissociated fluorescein concentration 2.64 mM). As the protonated HEPES molecules diffuse away from the uncaging site into the higher pH solution of the surrounding region, protons released from HEPES become available to subsequently bind to fluoresceins and reduce their fluorescence. A typical experimental record in a thin film of perfusate is shown in Fig. 2 (top).

The HEPES diffusion coefficient at 37°C, determined by fitting equation 1 to the data, was $5.1 \pm 0.76 \times 10^{-6}$ cm$^2$/sec ($n = 21$), about 65% of that expected for HEPES in free solution (free solution diffusion coefficient at 37°C based on MW of HEPES should be $7.9 \times 10^{-6}$ cm$^2$/sec). Other thin film experiments showed that the apparent HEPES diffusion coefficient was significantly smaller if the bulk solution pH fell below 7.0.

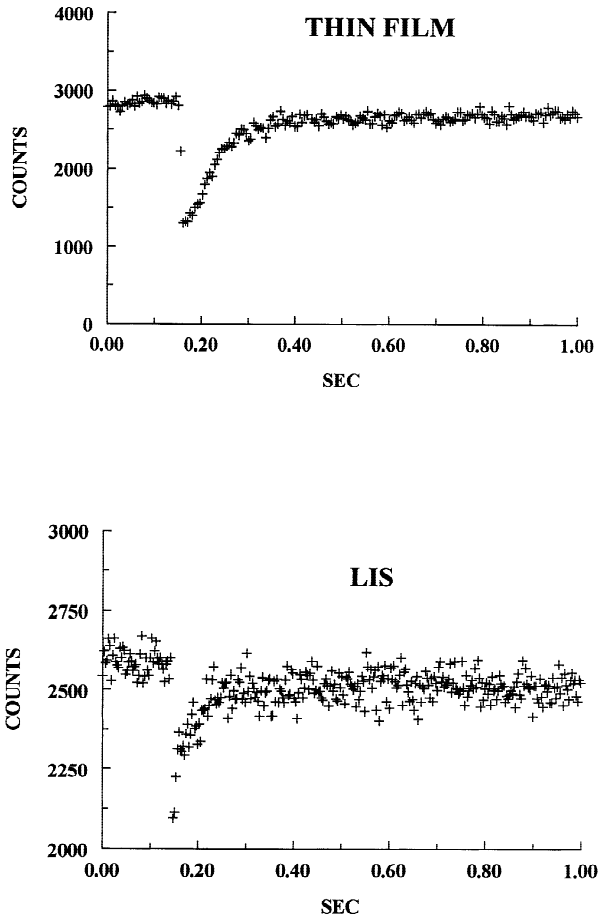


**Fig. 2.** Uncaging protons. The top panel shows a record of uncaging protons from the PMT channel corresponding to the site for uncaging protons in a thin film on a glass slide. The solution consisted of a 1-mM HEPES buffered solution with 0.5 mM NPE-caged protons and 0.5 mM fluorescein-70,000-MW dextran. The uncaging pulse at 0.15 sec releases protons that bind to HEPES and diminish the fluorescence of the fluorescein dextran. As the protonated HEPES diffuses away from the release site, the fluorescence increases toward the pre-uncaging value. The bottom panel shows a similar experiment in the LIS of MDCK cell epithelium.

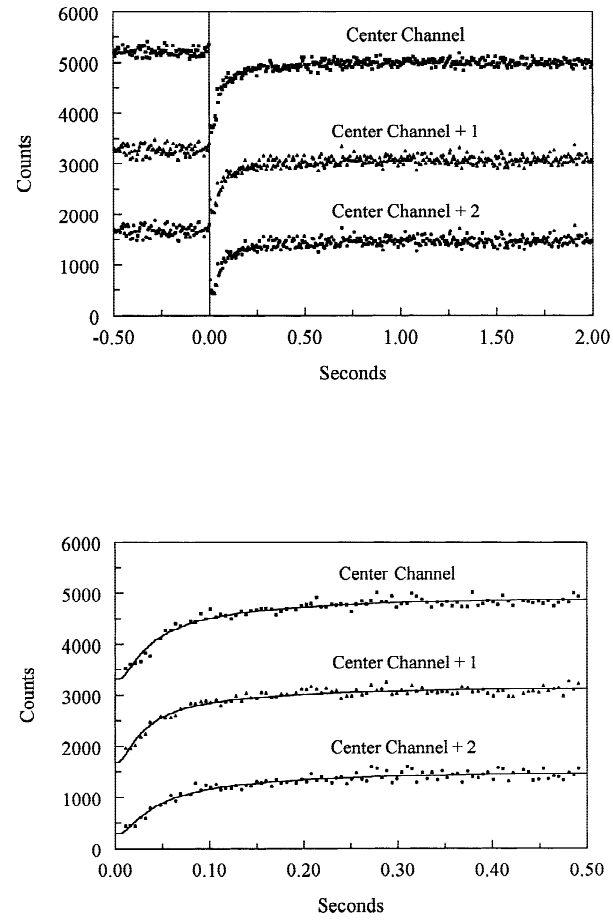


**Fig. 3.** Multichannel records of fluorescence from uncaging of protons in a thin film. The top panel shows records from three PMTs. Center Channel corresponds to the PMT at the uncaging site. The Center Channel + 1 represents the adjacent PMT record. The Center Channel + 2 represents the region two channels away from the uncaging site. The bottom panel shows nonlinear least square curves drawn to fit the data from the first 0.5 sec of the upper records.

We were concerned that the rate of HEPES movement in the thin film experiments, measured at the uncaging site, could have been slowed as a consequence of the low pH at that site. Therefore, we analyzed the signals from other PMT channels adjacent to the uncaging site. Figure 3 (top) shows a record of uncaging in a thin film from the PMT channel corresponding to the uncaging site (denoted Central Channel), the adjacent PMT in the horizontal direction (designated Central Channel + 1), and the next PMT (Central Channel + 2). Each PMT channel corresponds to a distance of 10 μm in the object; the uncaging site is located in the middle of the Central Channel, approximately 5 μm from the boundary with the second channel. The boundary of the third channel is then about 15 μm from the site of uncaging. Figure 3 (bottom) shows an example of the curve fits of Eq. 1 for all three PMT channels. The mean ± SEM HEPES diffusion coefficient calculated from the data from the second PMT adjacent to that at the uncaging site was $5.05 \pm 0.85 \times 10^{-6}$ cm$^2$/sec ($n = 21$), not significantly different from that determined at the uncaging site. The HEPES diffusion coefficient calculated for the third channel (Central Channel + 2) was $2.48 \pm 0.31 \times 10^{-6}$ cm$^2$/sec ($n = 16$), not significantly different from the values obtained from either of the adjacent channels. Thus, we conclude that the HEPES diffusion coefficient was not underestimated because of local reductions in medium pH.

Figure 2 (bottom) shows a typical experiment for the determination of HEPES diffusion in the LIS of MDCK cells. The HEPES diffusion coefficient was determined by fitting Eq. 2 to the data from the PMT corresponding to the uncaging site. The mean ± SEM HEPES diffusion

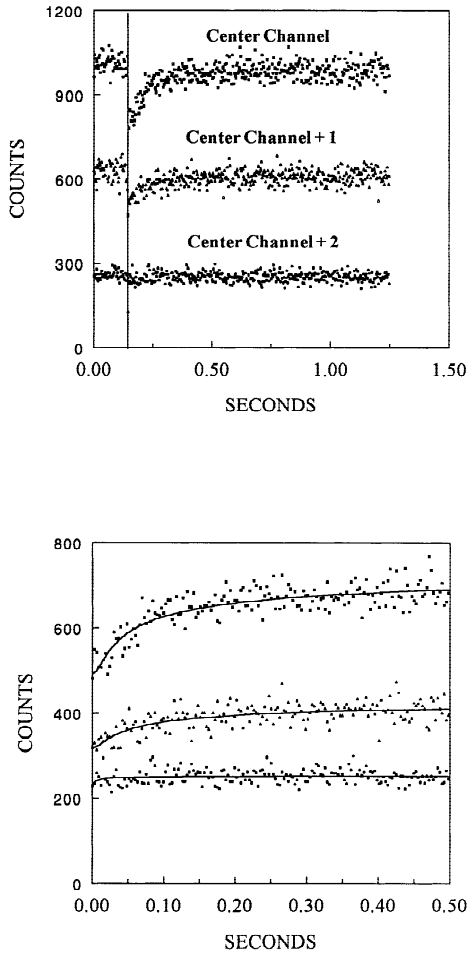


**Fig. 4.** Multichannel records of fluorescence from uncaging of protons in the LIS. The top panel shows records from three PMTs. Center Channel corresponds to the PMT at the uncaging site. The Center Channel + 1 represents the adjacent PMT record. The Center Channel + 2 represents the region two channels away from the uncaging site. The bottom panel shows nonlinear least square curves drawn to fit the data from the first 0.5 sec of the upper records. The curve fit to the Center Channel + 2 was not statistically significantly different from a straight line.

coefficient in the LIS at 37°C was 7.0 ± 0.88 × $10^{-6}$ $cm^2$/sec ($n = 16$), not significantly different from that measured in thin films or from that calculated for HEPES in free solution.

Analysis of the records from adjacent PMT channels was performed where possible, but the lower signal amplitude and poorer signal/noise of the data from the LIS precluded curve fitting most of the adjacent channels. Figure 4 (top) shows an example of the data obtained from the uncaging site (Central Channel) and the two adjacent horizontal channels. Figure 4 (bottom) shows the curve fit of Eq. 2 to the experimental data. The mean ± SEM of the diffusion coefficient from the adjacent channel (Central Channel + 1) was 3.3 ± 0.59 × $10^{-6}$ $cm^2$/sec ($n = 6$), while that from the next channel (Central Channel + 2) was 3.75 ± 2.3 × $10^{-6}$ $cm^2$/sec ($n = 2$). While neither value differed statistically from the obtained from the uncaging site, the low number of acceptable curve fits precluded more meaningful comparisons.

The fact that the HEPES diffusion coefficients determined from measurements of the uncaging site in the LIS and thin films did not differ significantly from one another or from that expected for free solution diffusion leads us to conclude that the movement of HEPES is not impeded in the LIS and that the diffusion of protons must be considerably faster than that of HEPES. The calculated hindrance factor for HEPES in the LIS was 0.73 ± 0.15, not significantly different from 1.0.

### 10 K Dextran Diffusion in the LIS by Fluorescence Recovery After Photobleaching

We wanted to determine whether the restriction to diffusion of the 10,000-MW fluorescein dextran in the LIS was due to the presence of glycocalyx within the LIS. Previously, such a mechanism for restriction of large solute diffusion in the LIS had been postulated from experiments on cells grown on glass coverslips (Xia et al., 1998). Reduction of the size of the glycosylation groups would be expected to increase the diffusivity of the dextran in the LIS. To diminish the glycocalyx, neuraminidase, an enzyme that cleaves terminal sialic acid residues from glycosylation chains, was mixed with the caged 10,000-MW fluorescein dextran and microinjected subepithelially as described in Materials and Methods. Surprisingly, all of the 'caged' dye in the LIS fluoresced brightly as if the caging groups had been removed. Subsequent experiments in solution showed that neuraminidase rapidly cleaved the dimethoxynitrobenzyl caging groups off the fluorescein moieties. We, therefore, determined the diffusivity of the dextrans in the LIS using fluorescence recovery after photobleaching (FRAP) as previously described (Harris et al., 1994).

The diffusivity of 10,000-MW fluorescein dextran, measured by FRAP, was significantly increased when the dye was injected into the LIS together with neuraminidase (2 mg/ml) compared to that of the dye alone. The ratio of diffusivity of the dextran within the LIS with enzyme ($n = 10$) to that without ($n = 6$) was 1.8 ± 0.68 (significantly greater than 1.0, $P < 0.05$). The enzymatically treated tissues exhibited a larger standard error than the control tissues and, although the number of observations was relatively small ($n = 10$), two populations appeared to be present. Four of the ten values were indistinguishable from the control while the other six were substantially larger. Although the low values could not be discarded on a statistical basis, we reasoned that they could represent cases of ineffective enzymatic digestion

of the glycocalyx. The diffusivity ratio calculated using only the 6 high values was 2.75. In either case, the restriction to diffusion of the 10,000-MW dextran was substantially relieved by neuraminidase and the hindrance factor calculated as the ratio of free solution diffusion compared to that in the presence of neuraminidase ranged between 1.98 and 3.0 depending on whether the low values were included in the neuraminidase group.

## Discussion

### Methodological Considerations

Recently, two-photon excitation has been employed to uncage calcium in the small volume defined by the two-photon cross section (Brown et al., 1999). While this approach has the virtue of confining the uncaging region in three dimensions, it results in the release of a very small quantity of calcium and requires 3-D analysis of its diffusional spread. We chose, as described previously (Xia et al., 1998), to avoid the complexity of analyzing the diffusional spread in three dimensions by utilizing an uncaging beam that was of uniform intensity and geometry in the axial direction. This approach simplified the mathematical analysis so that diffusion both in free solution and in the LIS could be analyzed in one dimension. Simultaneous imaging with an intensified CCD camera and quantitation by a multichannel PMT enabled the acquisition of high time resolution data while visually monitoring the quality of the uncaging and subsequent diffusion events. The good signal-to-noise and large dynamic range of the PMT detector were essential, particularly for the NPE-caged proton experiments. Although we analyzed the signals from several channels adjacent to the PMT at the uncaging site, we still did not fully exploit the capabilities of the multichannel PMT. Simultaneous records of photon counts were obtained from all channels but only one or a few were used for analysis. The full value of the device should become evident in multisite recording of fast events where the exact location of the events of interest is not known in advance.

We were not able to mathematically simulate the sequence of events involved in a proton uncaging experiment in a thin film or within the LIS when we used reasonable values for the reactant concentrations. The experimentally observed pH changes were much larger than the predicted ones, particularly in the thin film experiments. Clearly, some kinetic interactions must occur that could not be simulated using the reported pKs for HEPES and fluorescein-dextran. Within the LIS, the pH changes were smaller, as expected because of the buffering effects of the glycocalyx (Dzekunov & Spring, 1998), but even there our simulations were not quantitatively satisfactory. We were forced instead to compare the rates of diffusion of HEPES in the LIS to that experimentally measured in the thin film with the same reactant mixture. The lack of meaningful hindrance observed in the LIS was consistent with the data from HPTS and fluorescein-dextran uncaging experiments as well as those from earlier studies of MDCK cells on glass slides (Xia et al., 1998; Harris et al., 1994).

### Solute Diffusion Coefficients in the LIS

In our previous study of MDCK cell grown on glass coverslips, the hindrance factor for 10,000-MW fluorescein dextran had a value of 1.6, significantly higher than 1.0 but much less than the 5.6 value measured in cells grown on permeable supports. Smaller solutes showed virtually no restriction to their diffusion. This result is consistent with the conclusion that the slow diffusion of the 10,000-MW dextran in the LIS is the result of molecular hindrance rather than tortuosity of the lateral cell membranes. The experimental results after neuraminidase treatment indicate that the hindrance arises from the substantial glycocalyx that is known to be present on the lateral membranes of renal epithelial cells (Stow & Farquhar, 1987). Other tissues, (e.g., brain slices) exhibited restrictions to diffusion of 10,000-MW dextran and other large molecules that were attributed to tortuosity and local constrictions in the extracellular spaces rather than to glycosylation moieties (Nicholson & Tao, 1993).

One of the goals of this study was a determination of the diffusivity in the LIS of a small, monovalent cation. Restrictions to diffusion of cationic solutes might occur because of interaction with the fixed negative charges in the glycocalyx and cell membrane (Esposito et al., 1983; Junge & McLaughlin, 1987; Schnitzer, 1988). The only available caged monovalent inorganic cation, $H^+$, has the disadvantages of being the most mobile of all solutes and of reacting rapidly with a wide range of buffers. The diffusion measurements then represent the movement of protonated HEPES rather than of protons, per se. Our results showed that the rate of diffusion of HEPES in the LIS was extremely rapid and not different from that in free solution, from which we conclude that other smaller neutral or anionic solutes should move freely in this space and that restrictions in proton mobility are not detectable. Despite the above evidence for the free and rapid diffusion of small solutes within the LIS, we cannot completely rule out the possibility of a modest reduction in the mobility of monovalent cations, such as $Na^+$, in the LIS.

## References

Brown, E.B., Shear, J.B., Adams, S.R., Tsien, R.Y., Webb, W.W. 1999. Photolysis of caged calcium in femtoliter volumes using two-photon excitation. *Biophys. J.* **76:**489–499

Chatton, J.Y., Spring, K.R. 1994. Acidic pH of the lateral intercellular spaces of MDCK cells cultured on permeable supports. *J. Membrane Biol.* **140:**89–99

Dzekunov, S.M., Spring, K.R. 1998. Maintenance of acidic lateral intercellular spaces by endogenous fixed buffers in MDCK cell epithelium. *J. Membrane Biol.* **166:**9–14

Esposito, G., Faelli, A., Tosco, M., Orsenigo, M.N., Degasperi, R., Pacces, N. 1983. Influence of the enteric surface coat on the unidirectional flux of acetamide across the wall of rat small intestine. *Experientia* **39:**149–151

Harris, P.J., Chatton, J.Y., Tran, P.H., Bungay, P.M., Spring, K.R. 1994. pH, morphology, and diffusion in lateral intercellular spaces of epithelial cell monolayers. *Am. J. Physiol.* **266:**C73–C80

Junge, W., Mclaughlin, S. 1987. The role of fixed and mobile buffers in the kinetics of proton movement. *Biochim. Biophys. Acta* **890:**1–5

Kovbasnjuk, O.N., Leader, J.P., Weinstein, A.M., Spring, K.R. 1998. Water does not flow across the tight junctions of MDCK cell epithelium. *Proc. Natl. Acad. Sci. USA* **95:**6526–6530

Nicholson, C., Tao, L. 1993. Hindered diffusion of high molecular weight compounds in brain extracellular microenvironment measured with integrative optical imaging. *Biophys J.* **65:**2277–2290

Schnitzer, J.E. 1988. Glycocalyx electrostatic potential profile analysis: ion, pH, steric, and charge effects. *Yale J. Biol. Med.* **61:**427–446

Spring, K.R. 1999. Epithelial fluid transport — a century of investigation. *News in Physiol. Sci.* **14:**92–98

Spring, K.R. 1998. Routes and mechanism of fluid transport by epithelia. *Ann. Rev. Physiol.* **60:**105–119

Spring, K.R., Kovbasnjuk, O.N., Gibson, C.C., Bungay, P.M.. 1998. Application of a novel 8×8 PMT-array detector to light microscopy. *SPIE* **3261:**17–20

Stow, J.L., Farquhar, M.G.. 1987. Distinctive populations of basement membrane and cell membrane heparan sulfate proteoglycans are produced by cultured cell lines. *J. Cell Biol.* **105:**529–539

Xia, P., Bungay, P.M., Gibson, C.C., Kovbasnjuk, O.N., Spring, K.R. 1998. Diffusion coefficients in the lateral intercellular spaces of Madin-Darby Canine Kidney cell epithelium determined with caged compounds. *Biophys. J.* **74:**3302–3312